Cellular/Molecular

Actin Polymerization and ERK Phosphorylation Are Required for Arc/Arg3.1 mRNA Targeting to Activated Synaptic Sites on Dendrites

Fen Huang,[1] Jennifer K. Chotiner,[1] and Oswald Steward[1,2,3]

Departments of [1]Anatomy and Neurobiology, [2]Neurobiology and Behavior, and Neurosurgery, Reeve-Irvine Research Center, and [3]Center for the Neurobiology of Learning and Memory, University of California at Irvine, Irvine, California 92697

The mRNA for the immediate early gene *Arc/Arg3.1* is induced by strong synaptic activation and is rapidly transported into dendrites, where it localizes at active synaptic sites. NMDA receptor activation is critical for mRNA localization at active synapses, but downstream events that mediate localization are not known. The patterns of synaptic activity that induce mRNA localization also trigger a dramatic polymerization of actin in the activated dendritic lamina and phosphorylation of extracellular signal-regulated kinase 1/2 (ERK1/2) throughout the postsynaptic cytoplasm. The local polymerization of actin in the activated dendritic lamina is of particular interest because it occurs in the same dendritic domains in which newly synthesized Arc/Arg3.1 mRNA localizes. Here, we explore the role of activity-induced alterations in the actin network and mitogen-activated protein (MAP) kinase activation in Arc/Arg3.1 mRNA localization. We show that actin polymerization induced by high-frequency stimulation is blocked by local inhibition of Rho kinase, and Arc/Arg3.1 mRNA localization is abrogated in the region of Rho kinase blockade. Local application of latrunculin B, which binds to actin monomers and inhibits actin polymerization, also blocked the targeting of Arc/Arg3.1 mRNA to activated synaptic sites. Local application of the MAP kinase kinase inhibitor U0126 (1,4-diamino-2,3-dicyano-1,4-bis[2-amino-phenylthio]butadiene) blocked ERK phosphorylation, and also blocked Arc/Arg3.1 mRNA localization. Our results indicate that the reorganization of the actin cytoskeletal network in conjunction with MAP kinase activation is required for targeting newly synthesized Arc/Arg3.1 mRNA to activated synaptic sites.

Key words: **LTP; synaptic plasticity; protein synthesis; dendrite; rat; dendritic mRNA; dendritic spines; immediate early genes; MAP kinase; signal transduction; cytoskeleton; dendritic transport; dentate gyrus**

Introduction

Increasing evidence suggests that the immediate early gene *Arc/Arg3.1* is critically involved in processes of synaptic plasticity that are induced by activity and some forms of behavioral memory (Tzingounis and Nicoll, 2006). Arc/Arg3.1 has been intriguing since its discovery because it reveals cellular mechanisms that are capable of bringing about synapse-specific modifications that depend on transcription and translation. Originally, Arc/Arg3.1 attracted attention because newly synthesized Arc/Arg3.1 mRNA was rapidly delivered throughout dendrites (Link et al., 1995; Lyford et al., 1995). Later studies revealed that patterns of synaptic activity that trigger long-term potentiation (LTP) also caused Arc/Arg3.1 mRNA and protein to localize selectively at active synapses (Steward et al., 1998; Moga et al., 2004) and that this targeting depended on NMDA receptor activation (Steward and Worley, 2001b,c). Other studies revealed that induction of Arc/Arg3.1 expression is critical for both LTP and behavioral memory (Guzowski et al., 1999, 2000; Plath et al., 2006). Most recently, it has been found that Arc/Arg3.1 protein plays a critical role in cell biological processes that mediate glutamate receptor endocytosis (Chowdhury et al., 2006; Rial Verde et al., 2006; Shepherd et al., 2006; Tzingounis and Nicoll, 2006).

Localization of Arc/Arg3.1 mRNA at active synapses may be one of the critical events that must occur for the kinds of enduring synaptic modifications that underlie some forms of memory (Tzingounis and Nicoll, 2006). The mechanisms underlying Arc/Arg3.1 mRNA targeting to activated synapses are not fully understood, but there are a priori reasons to suspect that the actin cytoskeleton plays a role. Filamentous actin is highly organized in dendritic spines (Matus et al., 1982) and the organization of the actin network is regulated by synaptic activity (Segal and Andersen, 2000; Okamoto et al., 2004). Other studies have revealed a tight correlation between increases in polymerized actin in dendritic spines and the conditions that lead to hippocampal LTP (Lin et al., 2005; Kramar et al., 2006).

High-frequency stimulation (HFS) of the perforant path *in vivo* induces striking actin polymerization in the zone of the activated synapses, revealed by phalloidin staining (Fukazawa et al., 2003). This is the same dendritic region in which Arc/Arg3.1 mRNA localizes in response to HFS, raising the possibility that

Received Jan. 5, 2007; revised July 5, 2007; accepted July 5, 2007.

This work was supported by National Institutes of Health Grant NS12333 and a grant from FRAXA to O.S. J.K.C. was supported by Institutional National Research Service Award NS-07486. We thank Josephine Nguyen for excellent technical assistance.

Correspondence should be addressed to Dr. Oswald Steward, 1105 Gillespie Neuroscience Research Facility, 837 Health Sciences Drive, University of California at Irvine, Irvine, CA 92697. E-mail: osteward@uci.edu.

DOI:10.1523/JNEUROSCI.2410-07.2007

 0270-6474/07/279054-14$15.00/0

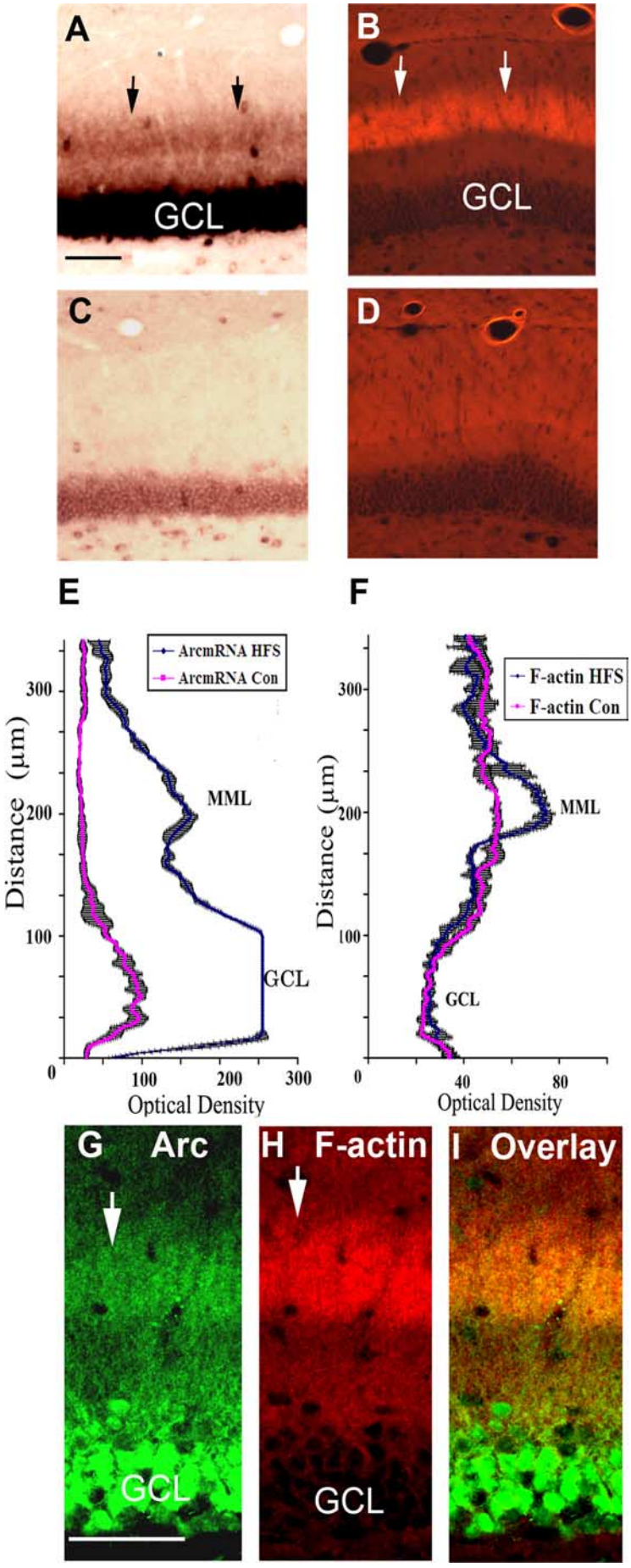

actin polymerization may be part of the molecular mechanism that underlies the targeting Arc/Arg3.1 mRNA to active synapses.

Here, we explore this hypothesis by assessing the relationship between changes in the actin network at active synapses and the targeting of Arc/Arg3.1 mRNA. We show that actin polymerization induced by HFS of the perforant pathway requires NMDA receptor activation, and depends on Rho kinase (ROCK). Pharmacological inhibition of Rho kinase or disruption of the actin cytoskeleton with latrunculin B blocked localization of Arc/Arg3.1 mRNA at active synaptic sites. Arc/Arg3.1 mRNA localization is also prevented by pharmacological blockade of extracellular signal-regulated kinase (ERK) phosphorylation, indicating that the local polymerization of actin and ERK phosphorylation are critical components of the mechanism that mediates the specific localization of Arc/Arg3.1 mRNA at active synaptic sites.

Materials and Methods

Neurophysiological techniques and stimulation paradigms. Our experiments took advantage of the unique model system provided by the perforant path projections to the dentate gyrus in rats, which terminates in a sharply defined lamina on the dendrites of granule cells. HFS of these projections induces LTP and triggers a host of molecular processes that have been characterized in previous studies (Steward et al., 1998; Steward and Halpain, 1999; Davis et al., 2000; Fukazawa et al., 2003).

For the present experiments, adult male Sprague Dawley rats were anesthetized with urethane (0.2 g/100 g body weight, by i.p. injec-

←

Figure 1. Arc/Arg3.1 mRNA localizes in the same dendritic lamina marked by the band of polymerized actin. ***A***, Selective localization of Arc/Arg3.1 mRNA in the middle molecular layer of the dentate gyrus in a rat that received repeated 400 Hz trains for 90 min. ***B***, Phalloidin staining reveals the band of polymerized actin in the middle molecular layer of the dentate gyrus from the same experiment. ***C***, ***D***, Arc/Arg3.1 mRNA expression (***C***) and phalloidin staining (***D***) for polymerized actin in the dentate gyrus contralateral to the HFS. The stimulated and control figures are from the same sections. ***E***, The graph illustrates OD measurements of Arc/Arg3.1 mRNA expression across the molecular layer in the areas illustrated in ***A*** (Arc/Arg3.1mRNA HFS) and ***C*** (Arc/Arg3.1mRNA Con). ***F***, Optical density measurements of phalloidin staining across the molecular layer in ***B*** and ***D***. ***G–I***, Colocalization of Arc/Arg3.1 protein and F-actin in the activated dendritic lamina. ***G***, Fluorescence immunocytochemistry for Arc/Arg3.1 protein in an animal that received repeated HFS. ***H***, Phalloidin staining for F-actin in the same section. ***I***, Overlay of Arc/Arg3.1 and F-actin. Arrows indicate the band of Arc protein (***G***) and polymerized actin (***H***) in the middle molecular layer. GCL, granule cell layer. Arrows point out the middle molecular layer, which has been activated. Scale bars, 100 μm.

tion) and placed in a stereotaxic frame. A constant body temperature was maintained by placing animals on a water-jacketed heating pad throughout the experiment. A stimulating electrode was placed in the medial entorhinal cortex (EC) at the following coordinates: 4.0 mm lateral, 1.0 mm anterior to the λ suture, and ~3–4 mm deep to the cortical surface. A recording electrode (a pulled-glass micropipette) was positioned in the dentate gyrus at 3.5 mm posterior to bregma, and 1.6 mm lateral and ~3.0 mm below the cortical surface. The final positions of the stimulating and recording electrodes were adjusted by monitoring the electrophysiological response generated by stimulation of the entorhinal cortex. The micropipette recording electrodes were filled either with 0.9% saline or drugs as described further below.

For stimulation paradigms that induce Arc/Arg3.1 mRNA localization, stimulus intensity was adjusted so as to elicit a 1.5–3.0 mV population spike. Test stimulation was delivered to determine the baseline response amplitude, and then three bouts of 10 trains (eight pulses at 400 Hz) were delivered at a rate of 1/10 s. Ten test stimuli were delivered after each of the three bouts of 10 trains to assess the degree of LTP. Then, trains of high-frequency stimuli (eight pulses at 400 Hz) were delivered at a rate of one every 10 s for different periods as described in the Results.

For experiments involving local delivery of drugs to the hippocampus, the micropipette recording electrode was filled with the drug solutions, allowing the drug to diffuse from the pipette (Steward and Halpain, 1999; Steward and Worley, 2001b). The following agents were dissolved in saline and delivered locally by diffusion: latrunculin B (400 μg/ml; Sigma, St. Louis, MO) in 10%DMSO/saline, (+)-5-methyl-10,11-dihydro-5*H*-dibenzo[a,d]cyclohepten-5,10-imine hydrogen maleate (MK801; 10 mg/ml; Tocris Bioscience, Ellisville, MO) in saline, Rho kinase inhibitor in solution (1 mM in saline; Calbiochem, La Jolla, CA), 1,4-diamino-2,3-dicyano-1,4-bis[2-amino-phenylthio]butadiene (U0126; 100 μM, 10% DMSO in saline; Tocris Bioscience), and 2-(2-diamino-3-methoxyphenyl-4*H*-1-benzopyran-4-one (PD98059; 200 μM, 10% DMSO in saline; Calbiochem).

Preparation of tissue for in situ *hybridization and immunocytochemistry.* At the termination of the neurophysiological experiments, rats were deeply anesthetized and perfused with 4% paraformaldehyde in 0.1 M PBS, pH 7.4. Brains were removed and postfixed overnight in 4% paraformaldehyde/PBS. Brains were sectioned on a vibratome at 40 μm and stored in 1× PBS at 4°C. Sections containing the drug delivery sites and control sections far from the drug sites were selected for immunocytochemistry and *in situ* hybridization.

Immunocytochemistry. Free-floating sections were heat-treated at 95°C for 5 min for antigen retrieval. Sections were incubated in blocking buffer for 2 h at room temperature [10% normal goat serum (NGS) for polyclonal antibod-

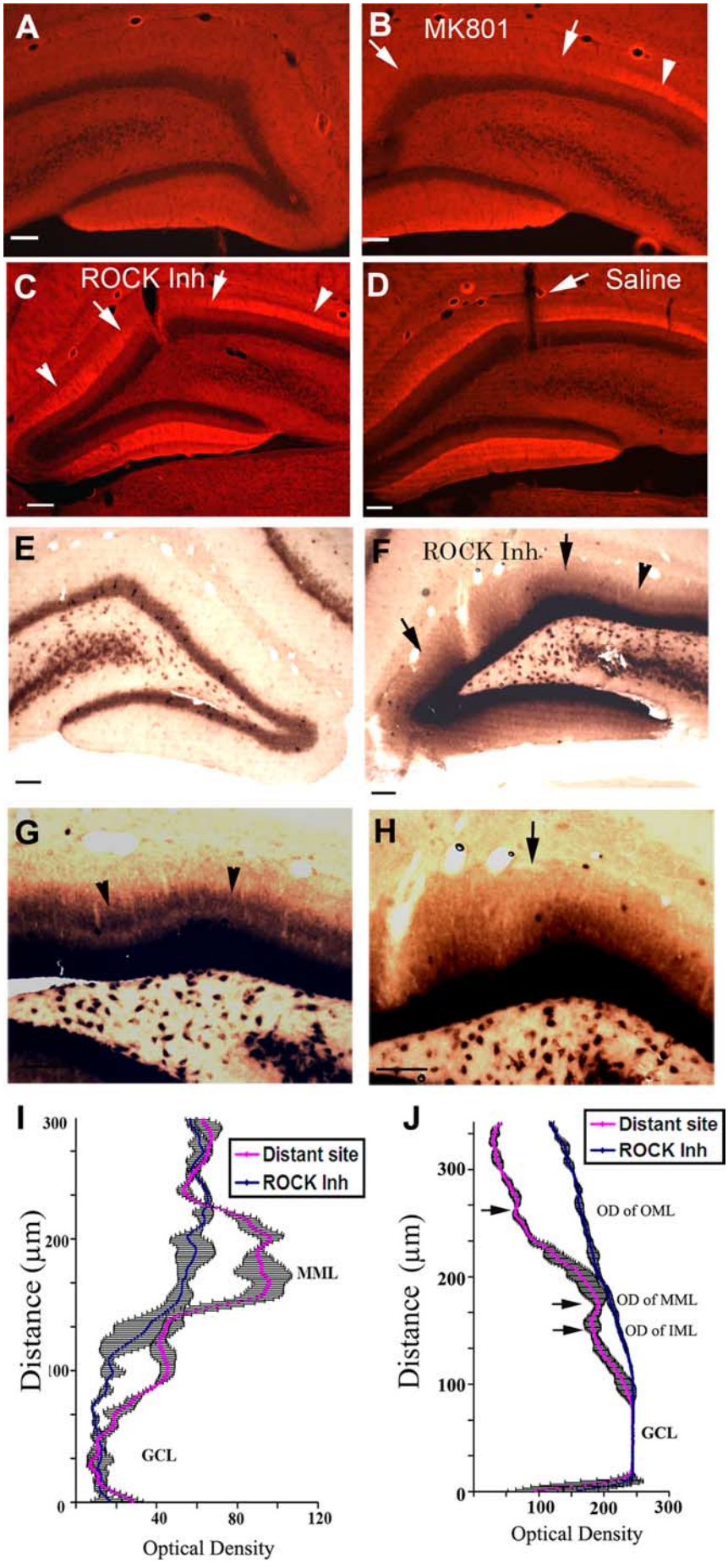

ies], then incubated with polyclonal phosphorylated ERK (p-ERK) antibody (catalog #9101; Cell Signaling Technology, Beverly, MA) at a dilution of 1:200 at room temperature overnight. Sections were washed with 1× TBS several times, and then incubated in biotin conjugated goat anti-rabbit IgG secondary antibody (1:500) for 2 h at room temperature. After washing, sections were incubated in Vector ABC kit (Vector Laboratories, Burlingame, CA) for 1 h, and then reacted with DAB and H_2O_2 for the colorization reaction. Sections were mounted on poly-L-lysine slides, dehydrated through alcohols to xylene, and coverslipped.

For double staining of p-ERK and Arc/Arg3.1, free-floating sections were heat-treated at 95°C for 5 min for antigen retrieval and were incubated in blocking buffer with goat polyclonal p-ERK antibody (1:200; catalog #sc-16982; Santa Cruz Biotechnology, Santa Cruz, CA) and rabbit polyclonal Arc/Arg3.1 antibody (1:1000; generous gift from Paul Worley, Johns Hopkins University, Baltimore, MD) at room temperature overnight. Goat anti-rabbit IgG-Alexa-488 and donkey anti-goat IgG-Alexa-546 were used for the detection of the primary antibodies. Sections were mounted on slides and coverslipped with ProLong Gold antifade reagent (Invitrogen, Eugene, OR).

The specificity of the primary antibody used here has been extensively documented. The polyclonal antibody for p-ERK recognizes bands at the expected molecular weights of ERK 1 and 2 in Western blots; antibody binding is seen only when the protein is phosphorylated (manufacturer's product information). The pattern of immunostaining for p-ERK provides strong validation for the specificity of the antibody because staining is strikingly altered by physiological activity (see Results).

For phalloidin staining, tissue sections were treated with PBS with 0.1% Triton X-100 for 30 min and then blocked with 2.5% BSA and 2.5% NGS/PBS for 2 h, and then incubated overnight at 4°C with phalloidin-tetramethylrhodamine isothiocyanate (TRITC) conjugate (0.5 μg/ml; Sigma). After incubation, the sections were washed three times with 1× PBS and then rinsed in water once. Sections were mounted on slides and coverslipped with ProLong Gold antifade reagent (Invitrogen). Previous studies have confirmed that increases in phalloidin staining correspond to increases in polymerized actin as measured biochemically (Fukazawa et al., 2003).

For double staining for phalloidin and Arc/Arg3.1 immunocytochemistry, sections were treated with PBS with 0.1% Triton X-100 for 30 min and then blocked with 2.5% BSA and 2.5% NGS/PBS for 2 h, and then incubated overnight at room temperature with Arc/Arg3.1 antibody (1:1000; a generous gift from Paul Worley). Sections were then incubated with Alexa-488-conjugated goat anti-rabbit IgG and phalloidin TRITC conjugate (0.5 μg/ml; Sigma) for 2 h at room temperature to detect the Arc/Arg3.1 primary antibody and F-actin, respectively.

In situ *hybridization.* For *in situ* hybridization, floating sections were postfixed with 4% paraformaldehyde in 0.1 M PBS for 30 min, then rinsed with 0.5× saline-sodium citrate buffer (0.5× SSC, 0.1% DEPC treated) for 5 min. Sections were treated with proteinase K (1.25 mg/L) for 15 min, and rinsed again with 0.5× SSC (0.1% DEPC treated) for 10 min. The sections were incubated with 75 μl of prehybridization buffer (2× SSC, 25% formamide, 1% Denhardt's reagent, 10% dextran sulfate, 0.5 mg/ml heparin, 0.5 mg/ml yeast tRNA, and 0.25 mg/ml of denatured salmon sperm DNA) and incubated at 42°C for 2 h. After the prehybridization, sections were incubated in 450 μl of hybridization buffer with 2 μg of digoxigenin-cRNA probe for Arc/Arg3.1 mRNA (Steward and Worley, 2002b) overnight at 55°C. The next day, sections were washed with 2× SSC/10 mM EDTA twice (10 min each). The sections were treated with RNase A for 30 min, and then washed twice with 2× SSC/EDTA (10 min per wash). The stringency wash was 0.5× SSC/10 mM EDTA at 55°C for 2 h. After that, sections were washed with 0.5× SSC twice (10 min each at room temperature). Alkaline phosphatase conjugated anti-digoxigenin Fab fragment (1:10,000) was used to detect the hybridized probes. Nitroblue tetrazoleum/5-bromo-4-chloro-3-indolyl phosphate solution was applied overnight at 4°C to detect the alkaline phosphatase. Sections were then washed with 100 mM Tris-HCl, pH 8.5/1 mM EDTA three times, 10 min each, and rinsed with nanopure water twice. Sections were mounted on coated slides, air dried, and covered with Kaiser's glycerol jelly.

Optical density measurements. Labeling produced by *in situ* hybridization and immunocytochemistry was analyzed quantitatively by measuring optical density (OD) in activated versus control sites. This was accomplished either by measuring OD using an M4 microcomputer imagine device (MCID) or by analyzing images using public-domain image-processing program ImageJ.

Using the MCID system, OD measurements were taken in a series of 10 × 10 μm measuring boxes. A row of five separate rows of OD measurements were taken at 10 μm intervals from the granule cell layer to the molecular layer and the five OD values at each level were averaged. Graphs illustrate the average OD at each level of the molecular layer. Data are shown as the SD of the measures at a given level.

Using ImageJ, optical density measurements were obtained from 20-μm-wide rectangular selections that extend across the granule cell body layer and molecular layer. Optical density values were calculated by averaging individual pixel intensities from each row of pixels. Graphs illustrate the average OD from values of three rectangular selections. Error bars in the figures represent the SD.

Results

HFS of the perforant path triggers actin polymerization and Arc/Arg3.1 mRNA localization in the activated dendritic lamina.

Previous studies have documented that activation of the perforant path using stimulation parameters that induce LTP triggers several events in postsynaptic granule neurons including (1) Arc/Arg3.1 mRNA and protein localization in the activated dendritic lamina (Steward et al., 1998), and (2) rapid polymerization of actin in the activated dendritic lamina revealed by phalloidin staining (Fukazawa et al., 2003).

Our standard paradigm for inducing perforant path LTP involves the delivery of three bouts of 10 trains at 400 Hz (a total of 30 trains), delivering 10 test pulses between each bout of 10 trains to assess the extent of synaptic potentiation, and then

←

Figure 2. Actin polymerization depends on NMDA receptor and Rho kinase activation, and inhibition of actin polymerization blocks Arc/Arg3.1 mRNA localization. ***A*** and ***B*** illustrate phalloidin staining from an experiment in which a micropipette filled with MK801 was positioned in the dentate gyrus during the period of HFS. ***A***, Phalloidin staining on the control (unstimulated) side. ***B***, Phalloidin staining on the side that received HFS. The micropipette containing MK801 was located between the arrows. Note the band of polymerized actin in areas distant from the micropipette (arrowheads), and the absence of the band in the area surrounding the micropipette (arrows). ***C–J***, Phalloidin staining and *In situ* hybridization for Arc/Arg3.1 mRNA in experiments in which micropipettes filled with the Rho kinase inhibitor were positioned in the dentate gyrus during the period of HFS. In these experiments, three bouts of 10 trains of 400 Hz were delivered to induce LTP, and then 400 Hz were delivered at a rate of 1/10 s for an additional 30 min. The animal was killed ~50 min after the first high-frequency train. ***C***, Phalloidin staining reveals a blockade of actin polymerization in the area surrounding the micropipette filled with the Rho kinase inhibitor (arrows). Note the prominent band of polymerized actin in areas distant from the micropipette (arrowheads). ***D***, Phalloidin staining of a section showing a band of phalloidin staining surrounding the track of a saline filled electrode. ***E***, Distribution of Arc/Arg3.1 mRNA as revealed by *in situ* hybridization in the control dentate gyrus contralateral to the side that received HFS. ***F–H***, Arc/Arg3.1 mRNA targeting to the activated dendritic lamina is blocked by inhibition of Rho kinase. ***F***, Pattern of labeling for Arc/Arg3.1 mRNA in the area surrounding the micropipette with the Rho kinase inhibitor. Arrowheads indicate the band of Arc/Arg3.1 mRNA in the activated dendritic lamina in areas distant from the micropipette. In the area immediately surrounding the micropipette, Arc/Arg3.1 mRNA is distributed diffusely across the dendritic lamina rather than being localized in a band in the activated segment (arrows), which indicates the blockade of Arc/Arg3.1 mRNA targeting as a result of inhibition of Rho kinase. ***G***, High-magnification photomicrograph illustrating the localization of Arc/Arg3.1 mRNA in sections posterior to the drug application site. Note the band of Arc/Arg3.1 mRNA in the middle molecular layer of dentate gyrus (arrowheads). ***H***, High-magnification photomicrograph illustrating Arc/Arg3.1 mRNA distribution in the area surrounding the micropipette with the Rho kinase inhibitor. Arrows indicate the areas in which Arc/Arg3.1 mRNA targeting is blocked. Graphs in ***I*** and ***J*** illustrate the optical density measurement across the molecular layer in areas surrounding the micropipette filled with the Rho kinase inhibitor (ROCK Inh) and areas distant from the micropipette (Distant site). I) Optical-density measurements of phalloidin staining for F-actin are as shown in C. ***J***, Optical-density measurements of Arc/Arg3.1 mRNA distribution as shown in ***F***. GCL, granule cell layer. Scale bars, 100 μm.

delivering repeated 400 Hz trains at 1/10 s for different periods of time. Although a 30 train HFS protocol is sufficient to induce Arc/Arg3.1, selective targeting of the mRNA to the active dendritic lamina requires synaptic activity during the time that Arc/Arg3.1 mRNA is present in dendrites (30–60 min after the first HFS) (Steward and Worley, 2001). Figure 1 illustrates an experiment in which the animal received HFS for 90 min. In this situation, Arc/Arg3.1 mRNA was strongly induced, as revealed by massive labeling over the layer of granule cell bodies, and there was also a discrete band of labeling in the activated dendritic lamina (the middle molecular layer) (Fig. 1*A*). The localized band of labeling for Arc/Arg3.1 mRNA in the molecular layer was in the same location as the striking band of polymerized actin revealed by phalloidin staining (Fig. 1*B*.) Quantitative assessment of the optical density of Arc/Arg3.1 mRNA and F-actin across the molecular layer revealed the distinctness of the band in the middle molecular layer (Fig. 1*E*,*F*). Note that in Figure 1*E*, the Arc/Arg3.1 mRNA signal in the cell body layer is saturated on the stimulated side; however, optical density in the dendritic lamina is below saturation, allowing comparisons across the molecular layer and between the two sides.

Comparisons of the localized band of Arc/Arg3.1 mRNA and the band of polymerized actin in nearby sections suggest that the two are colocalized. Assessing colocalization by performing *in situ* hybridization for Arc/Arg3.1 mRNA and phalloidin staining for F-actin in the same section has not been feasible in our hands, however, because of the differences in tissue preparation. Thus, to address the issue of colocalization, we took advantage of the fact that Arc/Arg3.1 protein accumulates in the activated dendritic lamina in the same pattern as Arc/Arg3.1 mRNA (Steward and Worley, 2001a) so that the distribution of Arc/Arg3.1 protein can be used as a proxy for the distribution of Arc/Arg3.1 mRNA. Double staining of individual sections for Arc/Arg3.1 protein and phalloidin revealed that the band of Arc/Arg3.1 protein and F-actin are colocalized in the same dendritic region (Fig. 1*G–I*). The colocalization of the band of phalloidin staining and the zone in which Arc/Arg3.1 mRNA localizes suggests the hypothesis that local polymerization of actin may be part of the mechanism underlying the localization of Arc/Arg3.1 mRNA in the activated dendritic lamina.

Actin polymerization depends on NMDA receptor activation

Previous studies have shown that local delivery of NMDA receptor antagonists block the induction of Arc/Arg3.1 mRNA transcription and targeting to dendrites that occurs after HFS of the perforant path (Steward and Worley, 2001b; Fukazawa et al., 2003). Systemic delivery of NMDA receptor antagonists has also been shown to block actin polymerization induced by HFS of the perforant path (Fukazawa et al., 2003). We confirmed this result in the present experiments by delivering the NMDA receptor antagonist MK801 by diffusion from the recording electrode, which blocks NMDAR in a small area in the dentate gyrus. Consistent with the findings of Fukazawa et al. (2003), actin polymerization was completely blocked in the region surrounding the MK801-filled micropipette (Fig. 2*B*). Similar results were seen in three separate experiments.

It should be noted that there is a very light band of increased phalloidin staining in the dentate gyrus on the side contralateral to the stimulation (Figs. 1*D*, 2*A*), which is not seen in control animals that did not receive perforant-path stimulation (data not shown). This light band probably reflects the activation of the sparse, crossed temporodentate pathway from the stimulated entorhinal cortex to the contralateral dentate gyrus.

Inhibition of Rho kinase blocks HFS-induced actin polymerization

What signaling pathways are responsible for actin polymerization induced by HFS? A likely candidate is the Rho family of small GTPases, including RhoA, Rac, and Cdc42, which has been shown to regulate different aspects of actin organization in various cell types including neurons (Hall, 1998; Luo, 2002). ROCK is a well characterized downstream effector of RhoA, and there is evidence that actin dynamics in dendrites and spines is mediated by this signal-transduction pathway (Tashiro and Yuste, 2004; Schubert et al., 2006).

Accordingly, we explored whether the actin polymerization induced by HFS was mediated by RhoA–Rho kinase. We used a highly selective and potent Rho kinase inhibitor (catalog #555550; Calbiochem) to selectively block Rho kinase activity. As with NMDA receptor antagonists, the inhibitor was delivered locally to the molecular layer of dentate gyrus by allowing it to diffuse from a recording micropipette electrode. Figure 2*C–J* illustrates an experiment in which three bouts of 10 400 Hz trains were delivered interspersed with 10 test stimuli, and then high-frequency trains were delivered at a rate of 1/10 s for 30 min. The rat was then perfused within ~3–4 min after the end of the stimulation (which was ~50 min after the first HFS train). As illustrated in Figure 2*C*, the band of increased phalloidin staining in the activated dendritic lamina was blocked in a small area surrounding the Rho kinase inhibitor-filled micropipette. Optical density quantification revealed that phalloidin staining intensity in the area surrounding the Rho kinase inhibitor-filled micropipette was significantly different from sites distant from drug application in the same section (Fig. 2*C*,*I*). Similar results were repeated in four experiments. To obtain a quantitative measurement of activity-induced actin polymerization and the blockade produced by the Rho kinase inhibitor, the OD at the peak of labeling in the middle molecular layer was compared with the OD in the side band regions proximal and distal to the band of polymerized actin. The average of 10 OD values at the peak of labeling in the middle molecular layer (MML) and 10 OD values in the inner molecular layer (IML) and outer molecular layer (OML) just proximal and distal to the band were calculated (Fig. 2*I*), and OD value difference was then calculated as OD MML − [(OD IML + OD OML)/2]. This calculation was done for the area surrounding the Rho kinase inhibitor-filled micropipette and in regions distant from the pipette where the band of F-actin was localized (Fig. 2*I*). The same quantitative comparisons were performed in a total of three separate experiments. The average OD value difference in the sites distant from ROCK inhibitor application is 35.38 ± 1.06, whereas the average OD value difference in ROCK inhibitor application sites is 8.42 ± 1.16, indicating that the band of polymerized actin in the activated dendritic lamina was blocked in the area surrounding the Rho kinase inhibitor-filled micropipette.

The vehicle for the Rho kinase inhibitor in these experiments was saline, and actin polymerization induced by HFS is not affected in the region surrounding saline-filled micropipettes (Fig. 2*D*) (see also Huang et al., 2005). These results indicate a critical role for Rho kinase in the actin polymerization that is triggered by strong synaptic activation.

Inhibition of Rho kinase blocks Arc/Arg3.1 mRNA targeting to the activated dendritic lamina

The band of polymerized actin marks the region in which Arc/Arg3.1 mRNA accumulates in response to perforant path activation, suggesting the possibility that the reorganization of the actin cytoskeleton revealed by phalloidin staining is part of the mech-

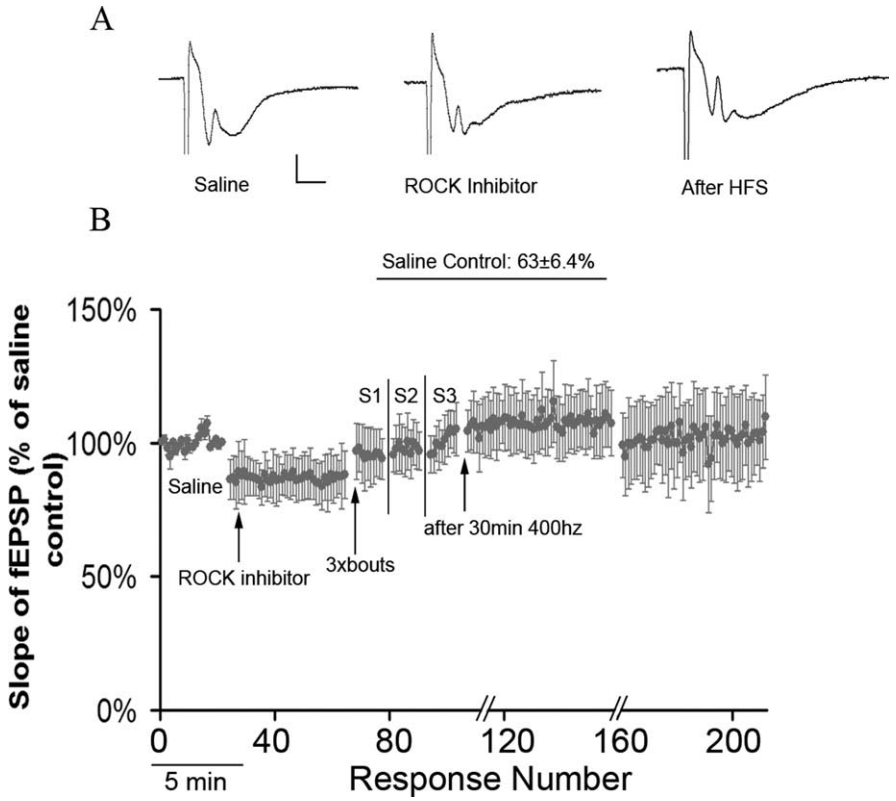

Figure 3. Inhibition of Rho kinase attenuates LTP. ***A***, Example traces of responses during baseline recording with a saline-filled electrode, after placement of the micropipette filled with the Rho kinase inhibitor, after the delivery of 3 × 10 400 Hz trains (S1, S2, and S3), and after 30 min of repeated delivery of 400 Hz trains at 1/10 s intervals. ***B***, The graph plots the average EPSP slope expressed as a percentage of the baseline across three separate experiments. Twenty-two test responses were collected with the saline-filled electrode; and forty test responses were collected after replacement of the Rho kinase inhibitor-filled electrode. After the baseline recording, three bouts of 400 Hz stimulation were applied and 10 test responses were taken after each bout. Then, continuous HFS was delivered for 30 min followed by 90 min of test stimulation to assess the extent of LTP. The graph shows the average EPSP slope of the first 50 responses after 30 min HFS and the last 50 responses before the end of the experiment. Note the slight drop of EPSP slope during the replacement of the saline-filled electrode with the Rho kinase inhibitor-filled electrode. EPSP slope increased by an average of 16% after three bouts of HFS, and by 23% after 30 min of continuous HFS, declining to 17% by the end of the testing period. In similar experiments with saline-filled micropipettes, the average percentage increase in field EPSP slope was 63 ± 6.4% (Steward and Worley, 2001b).

anism underlying the selective localization of Arc/Arg3.1 mRNA in activated dendritic domains. To test this hypothesis, we assessed whether blockade of actin polymerization by the Rho kinase inhibitor also blocked Arc/Arg3.1 mRNA localization. Sections from the same experiments in which we showed the blockade of F-actin by the Rho kinase inhibitor were stained for Arc/Arg3.1 mRNA by *in situ* hybridization. The site of blockade of actin polymerization in one case is illustrated in Fig. 2*C*. Inhibition of Rho kinase did not block Arc/Arg3.1 transcription or delivery of Arc/Arg3.1 mRNA into dendrites. Arc/Arg3.1 mRNA was induced and newly synthesized Arc/Arg3.1 mRNA was transported into dendrites in the area surrounding the micropipette. Importantly, however, Arc/Arg3.1 mRNA did not localize selectively in the activated lamina, and instead, remained diffusely distributed throughout the molecular layer of the dentate gyrus, indicating distribution of the mRNA throughout dendrites (Fig. 2*F*,*H*). Optical-density measurement across the molecular layer confirms the difference in Arc/Arg3.1 mRNA distribution pattern in the Rho kinase inhibitor application sites versus sites distant from the drug application on the same section (Fig. 2*F*,*J*).

To obtain a quantitative measurement of the accumulation of Arc/Arg3.1 mRNA in the activated dendritic lamina, and the blockade produced by the Rho kinase inhibitor across different experiments, similar quantification methods as for F-actin was used. Briefly, the OD at the peak of labeling in the middle molecular layer was compared with the OD in the side band regions proximal and distal to the band of labeling. The average of five OD values at the peak of labeling in the MML and five OD values in the IML and OML just proximal and distal to the band were calculated (Fig. 2*J*), and OD value difference was then calculated as OD MML − [(OD IML + OD OML)/2]. This calculation was done for the area surrounding the Rho kinase inhibitor-filled micropipette and in regions distant from the pipette where the band of Arc/Arg3.1 mRNA was localized (Fig. 2*J*). The same quantitative comparisons were performed in a total of three separate experiments. The average OD value difference in the sites distant from ROCK inhibitor application is 56.03 ± 5.15, whereas the average OD value difference in ROCK inhibitor application sites is 2.55 ± 0.65. As is evident, the selective localization of Arc/Arg3.1 mRNA in the activated dendritic lamina was completely blocked in the area surrounding the Rho kinase inhibitor-filled micropipette. These findings implicate actin polymerization triggered by HFS as an important part of the mechanism underlying the selective localization of Arc/Arg3.1 mRNA in the activated dendritic segment.

Inhibition of Rho kinase attenuates long-term potentiation induced by HFS of the perforant path

Given that inhibition of Rho kinase blocks actin polymerization and the targeting of Arc/Arg3.1 mRNA to activated dendritic segments, it was of interest to assess whether inhibiting Rho kinase affects perforant path LTP. To assess the physiological consequences of Rho kinase inhibition, a saline-filled electrode was first positioned in the molecular layer of the dentate gyrus to record the negative-going population EPSP (for example traces, see Fig. 3*A*). Baseline responses were recorded, and then the saline-filled micropipette was removed and replaced with a micropipette filled with the Rho kinase inhibitor, repositioning the electrode in the middle molecular layer of the dentate gyrus where the negative-going population EPSP was at its maximum. Single-pulse stimulation was then delivered to assess response amplitude and baseline responses were recorded for 30 min, and then three bouts of HFS (10 trains of eight pulses at 400 Hz) were delivered. Between each bout, 10 test pulses were collected to assess the degree of synaptic potentiation. After three bouts, high-frequency trains (eight pulses at 400 Hz) were delivered for another 30 min. After 30 min of HFS, test stimulation was delivered and test responses were recorded for 90 min to 2 h. In control experiments, the microelectrode was removed and replaced by another filled with saline.

Immediately after replacing the saline-filled micropipette by one filled with the Rho kinase inhibitor, responses evoked by

perforant path stimulation were reduced, and then recovered to an average of 86.9 ± 1.3%% of the baseline after a few minutes (Fig. 3*B*). This is within the range of what is seen when one saline electrode is replaced by another (Steward and Worley, 2001b). Immediately after three bouts of HFS, the slope of the negative-going EPSP was 16.1 ± 4.1% higher than the postdrug baseline response. Response amplitude remained elevated after 30 min of continuous HFS (23.8 ± 2.6%), and was still elevated 90 min after HFS (17.1 ± 3.9%), indicating that the LTP that was induced was long lasting. Nevertheless, the extent of the increase in EPSP slope was less than is typically seen. For example, in control experiments that used identical stimulation and recording techniques, the mean increase in slope of the negative-going population EPSP in five animals was 63 ± 6.4% immediately after delivery of the trains (Steward and Worley, 2001b). Thus, inhibition of Rho kinase attenuates the induction of LTP, but the LTP that does occur persists for the duration of the testing period.

In interpreting the residual potentiation seen here, it is important to recall that the population EPSP is a field response that reflects the summation of synaptic currents over some distance. Thus, the residual potentiation may reflect enhanced synaptic currents from locations outside the area of blockade of actin polymerization.

Actin polymerization inhibition with latrunculin B suppresses transcriptional activation of Arc/Arg3.1

The experiments above demonstrate that Rho kinase inhibition blocks actin polymerization and Arc/Arg3.1 mRNA targeting. It is possible, however, that blockade of Arc/Arg3.1 mRNA localization is not directly caused by the blockade of actin polymerization and instead reflects some other roles of Rho kinase. To further confirm the role of the actin cytoskeleton, we assessed the effects of latrunculin B, which binds to monomeric actin and reduces its availability, and thus shifts the equilibrium between polymerization and depolymerization toward net depolymerization. Previous studies have shown that latrunculin B disrupts F-actin in dendritic spines and also blocks the late phase of LTP (Allison et al., 1998; Fukazawa et al., 2003). As above, latrunculin B was delivered locally by allowing it to diffuse from a micropipette positioned in the dentate gyrus before delivering HFS to the perforant path. As shown in Figure 4, *A* and *B*, local delivery of latrunculin B completely blocked the development of the band of actin polymerization and also caused a loss of phalloidin staining in a small region surrounding the micropipette, as revealed by a loss of fluorescence in the area surrounding the latrunculin B-filled micropipette (Fig. 4*B*).

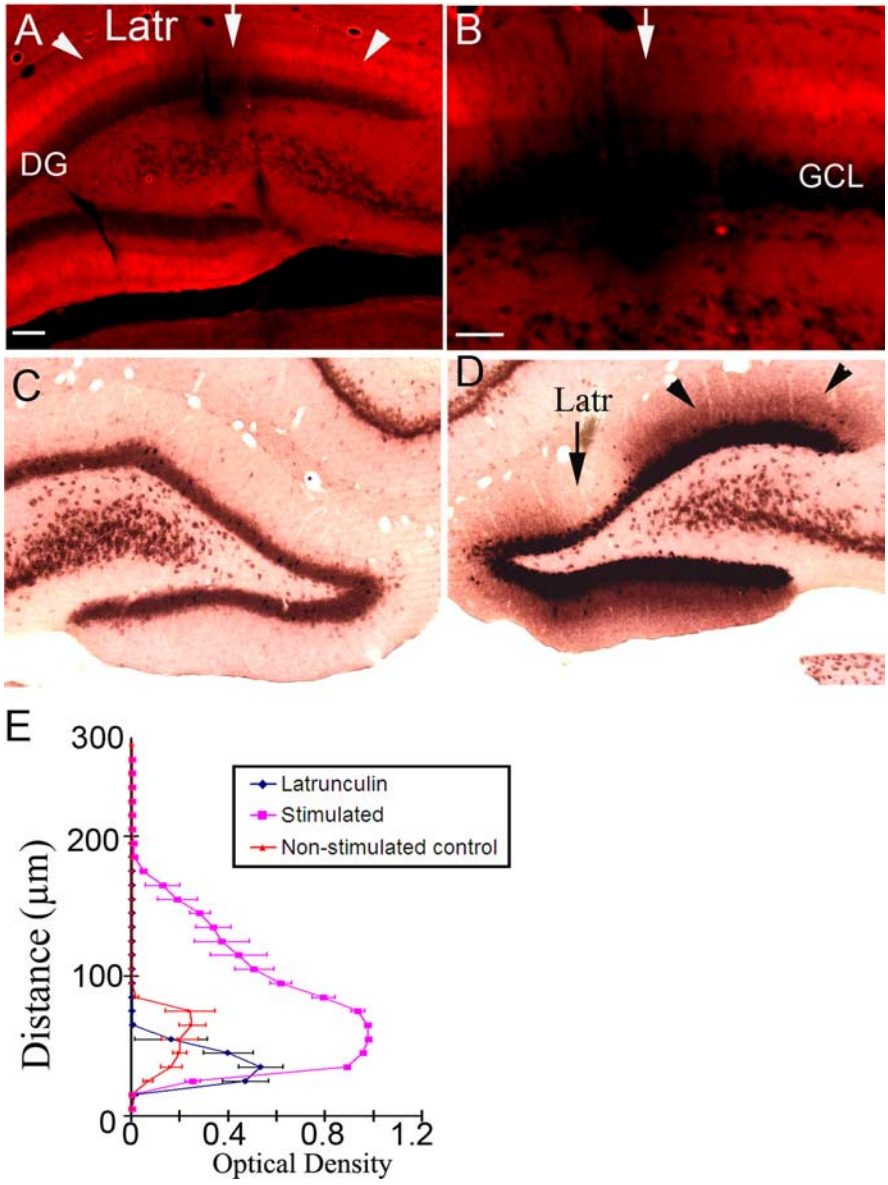

Figure 4. Latrunculin B blocks actin polymerization and Arc/Arg3.1 mRNA induction. ***A*** and ***B*** show an experiment in which micropipettes filled with latrunculin B (Latr) were positioned in the dentate gyrus during the period of HFS. In these experiments, HFS was delivered for 30 min. ***A***, Phalloidin staining reveals a blockade of actin polymerization in the area surrounding the micropipette filled with the latrunculin B (arrows). Note the prominent band of polymerized actin in areas distant from the micropipette (arrowheads). ***B***, High-magnification pictures of the pattern of phalloidin staining in the site of latrunculin B application. ***C–E***, Distribution of Arc/Arg3.1 mRNA in experiments in which micropipettes filled with latrunculin B were positioned in the dentate gyrus during the period of HFS. In these experiments, HFS was delivered for 90 min. ***C***, Arc/Arg3.1 mRNA expression in the dentate gyrus contralateral to HFS. ***D***, Arc/Arg3.1 mRNA expression in the area surrounding the latrunculin B-filled micropipette. Note the blockade of Arc/Arg3.1 mRNA induction in the area of latrunculin B application (arrow) and strong expression in areas distant from the site of drug application (arrowheads). ***E***, Plot of the average OD across the molecular layer from the case shown in ***A*** and ***B***. Pink represents the OD in the stimulated dentate gyrus, red illustrates OD values in the dentate gyrus on the control side contralateral to the stimulation, and blue represents the OD in the latrunculin B application site. Error bars indicate the SD of the five measurements at each level. Sti, Stimulation; DG, dentate gyrus; GCL, granule cell layer. Scale bar, 100 μm.

To assess whether latrunculin B also blocks Arc/Arg3.1 mRNA localization, latrunculin B-filled micropipettes were positioned in the dentate gyrus, and HFS was delivered for 90 min to induce Arc/Arg3.1 and cause the mRNA to localize in the activated lamina. In contrast to the Rho kinase inhibitor, Arc/Arg3.1 mRNA transcription was substantially inhibited in the area of decreased

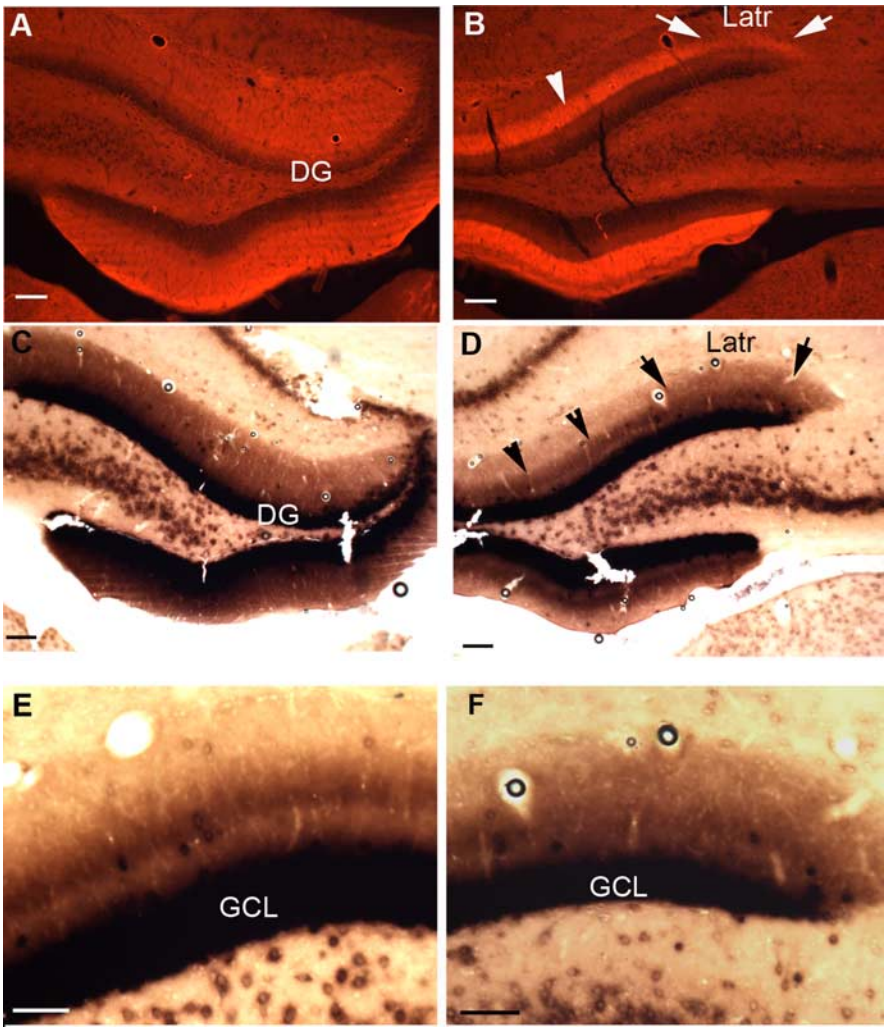

Figure 5. Latrunculin B blocks the targeting of Arc/Arg3.1 mRNA to active synaptic sites. ***A–D*** show an experiment in which the rat was given an ECS, followed by HFS of the perforant path on one side with a latrunculin B-filled recording micropipette positioned in the dentate gyrus. ***A***, Phalloidin staining in the dentate gyrus on the control side contralateral to HFS. ***B***, Phalloidin staining in the dentate gyrus on the side that received HFS of the perforant path with latrunculin B in the micropipette. Arrows point out the latrunculin B application site. Note the blockade of the band of phalloidin staining. ***C***, Arc/Arg3.1 mRNA expression in the dentate gyrus that received ECS only. Note that Arc/Arg3.1 mRNA is distributed uniformly across the molecular layer after induction by an ECS. ***D***, Arc/Arg3.1 mRNA induced by an ECS selectively localizes in the activated dendritic lamina after HFS except in areas of latrunculin B application. Arrows point out the latrunculin B application sites. Note the diffusive distribution of Arc/Arg3.1 mRNA in the drug sites and the absence of a band of labeling in the middle molecular layer. In areas distant from the drug site, Arc/Arg3.1 mRNA is selectively localized (arrowheads). ***E***, ***F***, High-magnification pictures of Arc/Arg3.1 mRNA localization in the site distant from the latrunculin B application and the site with drug application. Latr, Latrunculin B; GCL; granule cell layer; DG, dentate gyrus. Scale bars, 100 μm.

phalloidin staining. Some granule neurons did show increased levels of labeling for Arc/Arg3.1 mRNA, but the overall level of labeling was much less than in sites distant from the site of latrunculin B application (Fig. 4*D*). This was confirmed by optical density quantification (Fig. 4*E*). The different effects of the Rho kinase inhibitor and latrunculin B on Arc/Arg3.1 mRNA transcription may be explained by differences in the mechanisms of their inhibition of actin polymerization. For example, the Rho kinase inhibitor may block molecular pathways responsible for activity-induced actin polymerization, but not affect the maintenance of polymerized actin because it does not affect the balance between ongoing polymerization and depolymerization. In contrast, latrunculin B would disrupt both the activity induced and also the basal level of actin polymerization. For reasons yet to be established, this twofold effect may disrupt the molecular cascades required for Arc/Arg3.1 mRNA transcription.

Latrunculin B blocks targeting of Arc/Arg3.1 mRNA to active synapses

To assess whether latrunculin B also blocked targeting of the mRNA to active synapses, it was necessary to use a paradigm in which targeting could be assessed independently of the induction of transcription. Hence, we used the approach that we used previously to document a role for NMDA receptors in Arc/Arg3.1 localization in which transcription is induced by a generalized stimulus [an electroconvulsive stimulation (ECS)] and localization is then induced by stimulating the perforant path (Steward and Worley, 2001b). Rats were given an ECS to induce Arc/Arg3.1 mRNA expression and were then anesthetized and prepared for acute neurophysiology. A micropipette filled with latrunculin B was positioned in the dentate gyrus as in the experiments above ~1 h after the ECS; by this time, the Arc/Arg3.1 mRNA induced by the seizure had been transported throughout dendrites. Then, ~1 h and 30 min after the ECS, HFS was delivered to the perforant path to induce Arc/Arg3.1 mRNA targeting. In this situation, the Arc/Arg3.1 mRNA that was induced by the ECS rapidly relocalizes to the activated dendritic lamina (Steward and Worley, 2001b), as evidenced by a band of labeling for Arc mRNA in the in the same region as the band of polymerized actin (Fig. 5*B*,*D*). This relocalization was completely blocked in the area where latrunculin B blocked actin polymerization (Fig. 5, compare *B*, *D*, *F*). In the areas surrounding the micropipette, Arc/Arg3.1 mRNA was distributed uniformly across the dendritic lamina as on the contralateral side, in contrast to the band of labeling in areas distant from the micropipette on the side of the stimulation (Fig. 5, compare *E*, *F*). Similar results were seen in three experiments. This finding further confirms that actin polymerization is critical for Arc/Arg3.1 mRNA targeting to the activated synapses.

The band of polymerized actin is not sufficient to cause Arc/Arg3.1 mRNA to localize

The data above indicate that the reorganization of the actin network revealed by phalloidin staining is part of the mechanism that causes Arc/Arg3.1 mRNA to localize selectively. The question is whether it is sufficient. To address this question, we took advantage of the fact that the band of polymerized actin is highly stable once induced (Fukazawa et al., 2003), whereas Arc/Arg3.1 mRNA is no longer localized 4 h after the inducing stimulus. Rats were anesthetized with Nembutal, which produces transient anesthesia, and HFS was delivered to the perforant path for 30 min

to induce a band of polymerized actin in the activated lamina. Then, animals were removed from the stereotaxic apparatus and allowed to recover consciousness. Two hours after the cessation of stimulation, an ECS was induced to strongly activate Arc/Arg3.1 transcription, and animals were perfused 2 h later (which is 4 h after the termination of the HFS). Although the initial perforant path stimulation would strongly induce Arc/Arg3.1 and generate signals sufficient to cause the mRNA to localize in the activated lamina, Arc/Arg3.1 mRNA is no longer localized 4 h after the cessation of high frequency synaptic stimulation. If the band of polymerized actin induced by the original stimulation was sufficient to mediate mRNA localization, the Arc/Arg3.1 mRNA induced by the ECS would localize selectively in the area of the actin band (Fig. 6*B*). As illustrated in Figure 6*D*, this did not occur; instead, the Arc/Arg3.1 mRNA induced by the ECS was distributed uniformly across the molecular layer, as on the nonstimulated side (Fig. 6*C*). Optical density measurements reveal that there is no band of Arc/Arg3.1 mRNA localization in the HFS plus ECS side and no difference in Arc/Arg3.1 mRNA distribution on the stimulated and control side (Fig. 6*E*). Thus, the band of polymerized actin is not sufficient to cause Arc/Arg3.1 mRNA to localize, indicating that either the timing of the polymerization relative to the presence of Arc/Arg3.1 mRNA in the dendrite is critical for Arc/Arg3.1 mRNA localization or that some other signal is required in addition to the band of polymerized actin.

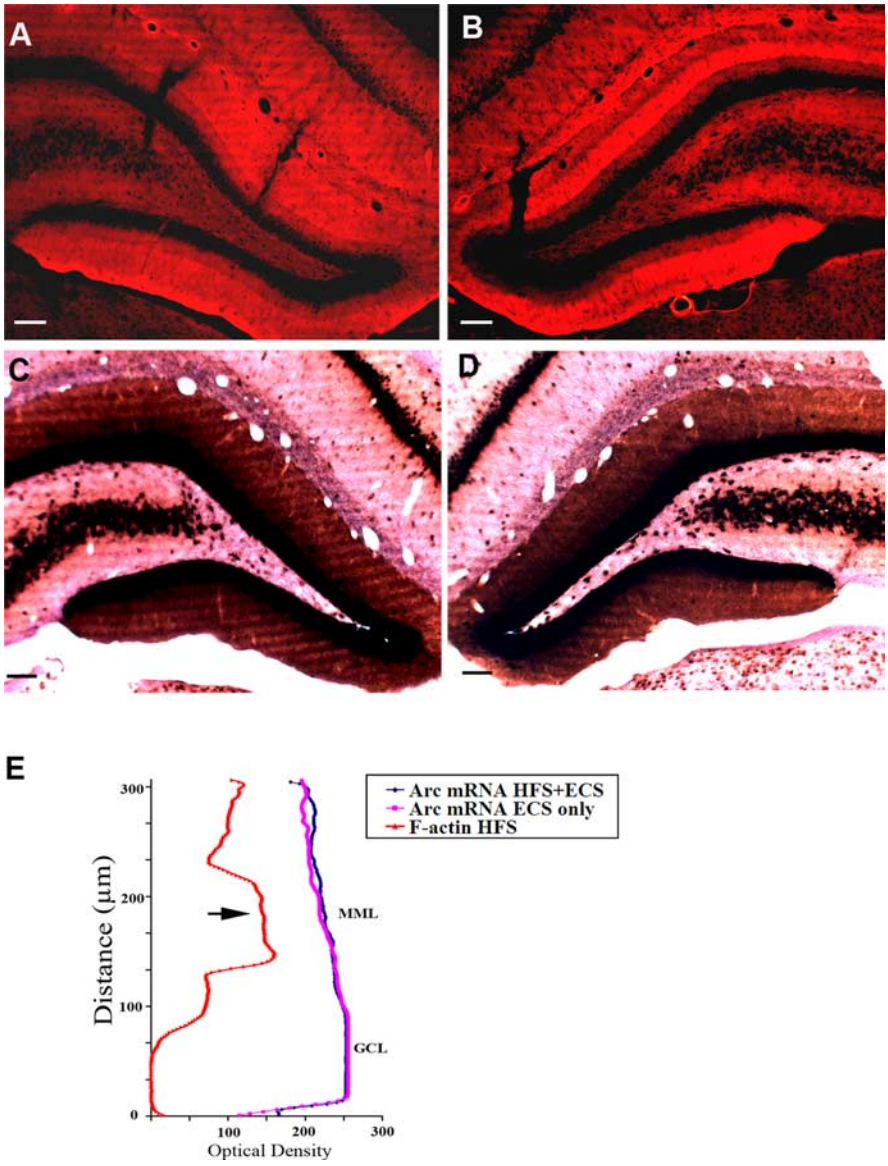

Figure 6. Actin polymerization alone is not sufficient for Arc/Arg3.1 mRNA targeting. ***A–D*** illustrate an experiment in which actin polymerization was induced by delivering HFS for 30 min to induce the band of polymerized actin. The rat was allowed to recover from the anesthesia, and then received an ECS 2 h after the cessation of HFS, which strongly activates Arc/Arg3.1 transcription. The rat was perfused 2 h after the ECS. ***A***, Control pattern of phalloidin staining in the dentate gyrus contralateral to the HFS. ***B***, Phalloidin staining in the dentate gyrus on the side of the stimulation. Note that the band of phalloidin staining is still evident 4 h after the cessation of HFS. ***C***, Arc/Arg3.1 mRNA distribution on the side of dentate gyrus contralateral to the HFS. Arc mRNA expression is strongly induced as a result of the ECS and Arc/Arg3.1 mRNA is distributed diffusely across the molecular layer. ***D***, Similarly, Arc/Arg3.1 mRNA induced by an ECS is also distributed diffusely across the molecular despite the presence of the band of polymerized actin. ***E***, Optical-density measurements of phalloidin staining in the dentate gyrus on the side that received HFS (red line) and Arc/Arg3.1 mRNA distribution in the dentate gyrus on both the side that received HFS (blue line) and on the control side with ECS only. Note the peak in the middle molecular layer for F-actin and the absence of any indication of higher levels of labeling for Arc/Arg3.1 mRNA in the middle layer on the HFS side compared with the side that received ECS only. Thus, the band of polymerized actin from previous synaptic activation is not sufficient to capture Arc/Arg3.1 mRNA induced by a seizure. Scale bars, 100 μm.

ERK phosphorylation is also required for Arc/Arg3.1 mRNA targeting to activated synaptic sites

One possible interpretation of the fact that a pre-existing band of polymerized actin is not sufficient to cause Arc/Arg3.1 mRNA to localize is that some other signal is required in addition to the band of polymerized actin. An important clue about the nature of the additional signal is that it does not persist several hours after stimulation, as shown by the fact that Arc/Arg3.1 mRNA induced by a seizure does not localize at a previously established band of polymerized actin (Fig. 6). One candidate is the dramatic phosphorylation of ERK1/2, which is induced by HFS of the perforant path (Davis et al., 2000).

To confirm that ERK1/2 was phosphorylated in response to the stimulation parameters used here, we stained tissue from animals that had received stimulation sufficient to induce Arc/Arg3.1 mRNA localization. In addition to the dramatic increase in immunostaining for p-ERK throughout the dendritic and cell body laminae shown previously (Davis et al., 2000), there was also a sharply defined band of even higher levels of immunostaining in the middle molecular layer (the site of termination of the synapses of the medial perforant path that had been strongly activated) (Fig. 7*B*), in the same location as the band of polymerized actin (Fig. 7*C*). Sections that were double-stained for p-ERK and Arc/Arg3.1 protein revealed that the band of enhanced p-ERK staining occurred in the same lamina as the band of enhanced staining for Arc/Arg3.1 protein, which is a surrogate measure of the location of the band of Arc/Arg3.1 mRNA (Fig. 7*D–F*).

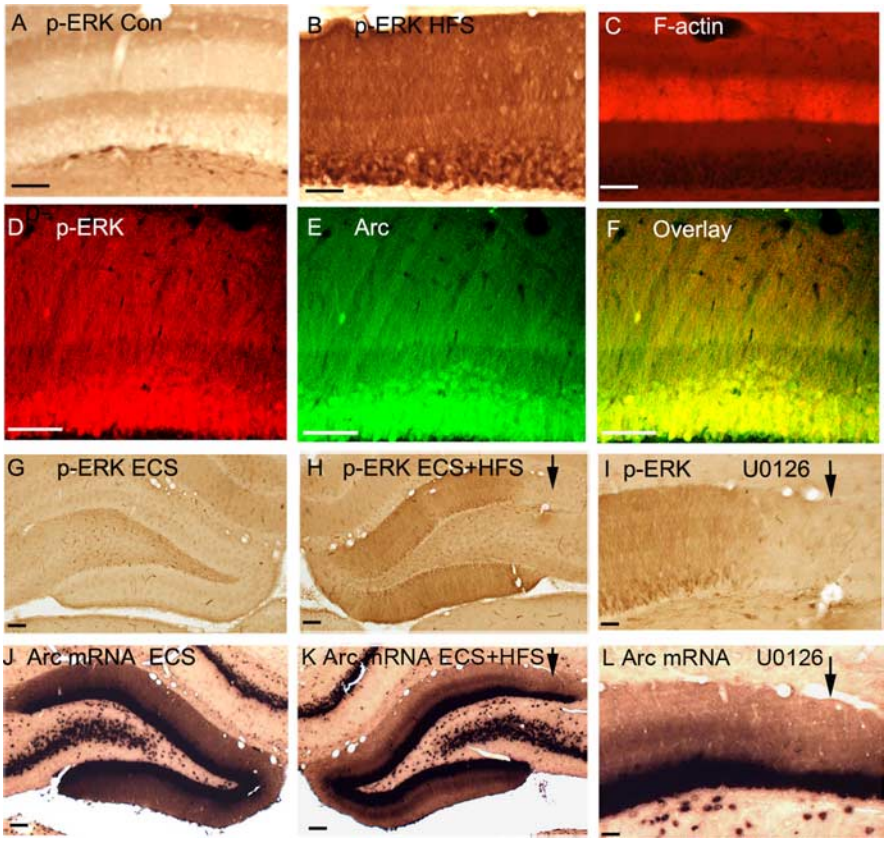

Figure 7. Blockade of ERK phosphorylation blocks the targeting of Arc/Arg3.1 mRNA to the activated dendritic lamina. ***A***, p-ERK immunostaining in the control dentate gyrus contralateral to the stimulated side. ***B***, p-ERK immunostaining in the dentate gyrus that received HFS. Note the massive ERK phosphorylation in dendrites and also the band of increased immunostaining in the middle molecular layer (arrow), which is in the same location as the band of polymerized actin (***C***). ***D–F*** show the colocalization of p-ERK and Arc/Arg3.1 protein in the activated dendritic lamina. ***D***, Fluorescence immunocytochemistry for p-ERK (red). ***E***, Fluorescence immunocytochemistry for Arc/Arg3.1 protein. ***F***, Overlay of Arc/Arg3.1 protein and p-ERK. ***G–L*** show an experiment in which Arc/Arg3.1 expression was induced by an ECS, and HFS was then delivered beginning 2 h after the ECS to induce localization in the activated dendritic lamina (Steward and Worley, 2001b). In this experiment, a micropipette filled with U0126 was present at the site indicated by the arrow. ***G*** and ***H*** illustrate p-ERK staining contralateral and ipsilateral to the stimulation. Note the blockade of ERK phosphorylation in the area surrounding the micropipette (arrows). ***I***, Higher-magnification view of the area of blockade. ***J***, Arc/Arg3.1 mRNA distribution on the side contralateral to the HFS. Arc/Arg3.1 mRNA that was induced by the ECS is distributed uniformly across the dendritic lamina. ***K***, On the side of the HFS, Arc/Arg3.1 mRNA is selectively localized in the activated dendritic lamina except in the area in which ERK phosphorylation is blocked (arrows). ***L***, Higher-magnification view of the area of blockade. Note that in the area of blockade, Arc/Arg3.1 mRNA is distributed uniformly across the dendritic lamina as on the contralateral side that did not receive HFS. Con, Control; GCL, granule cell layer. Scale bars, 100 μm.

This highly localized band of p-ERK in the activated dendritic zone is an attractive candidate as comediator (with actin polymerization) of Arc/Arg3.1 mRNA localization. This is especially true because ERK phosphorylation does not persist for more than ~45 min after the cessation of HFS, and would thus not be present in the capture experiment shown in Figure 6. The obvious way to test this hypothesis is to pharmacologically block ERK phosphorylation. A potential complication, however, is that ERK activation may be required for inducing Arc/Arg3.1 transcription (Waltereit et al., 2001). Accordingly, we used the same strategy that we used previously to document a role for NMDA receptors in targeting, in which Arc/Arg3.1 expression was induced by a generalized stimulus (a seizure) and HFS was then delivered to induce localization in the activated dendritic lamina (Steward and Worley, 2001b). For these experiments, rats received an ECS and were then anesthetized and prepared for neurophysiological recording. Beginning ~2 h after the seizure, at which time Arc/Arg3.1 mRNA is distributed throughout dendrites, saline-filled recording electrodes were placed and test responses were collected. Then the saline filled micropipette was replaced with a micropipette filled with U0126, test responses were again collected and stimulus intensity was adjusted if necessary, and HFS was delivered for 30 min to 1 h, which is sufficient to cause Arc/Arg3.1 that is distributed throughout dendrites to relocalize to the activated dendritic lamina (Steward et al., 1998). The prediction is that if U0126 blocks targeting, then Arc/Arg3.1 mRNA should remain distributed diffusely throughout dendrites instead of relocalizing in response to HFS.

As illustrated in Figure 7, U0126 did block Arc/Arg3.1 mRNA targeting as predicted. On the side contralateral to the stimulation, p-ERK staining was similar to the control except for the presence of a few neurons in the hilus that exhibited high levels of p-ERK immunostaining; any other induction caused by the ECS 2 h earlier had dissipated. In contrast, on the side that received HFS, there was massive induction of ERK phosphorylation except in the region surrounding the U0126-filled micropipette (Fig. 7*H*,*I*) (the area of blockade is indicated by the arrow). Arc/Arg3.1 mRNA was still strongly induced on the nonstimulated side as a result of the ECS, and as expected was distributed diffusely throughout the dendritic lamina (Fig. 7*J*). On the side that received HFS, Arc/Arg3.1 mRNA was localized in a band in the activated dendritic lamina (Fig. 7*K*) except in the area in which ERK phosphorylation was blocked (Fig. 7*K*,*L*) (the area of blockade is indicated by the arrow). In the area in which ERK phosphorylation was blocked, Arc/Arg3.1 mRNA was distributed diffusely across the dendritic lamina in the same way as on the side that received no stimulation (arrow). Similar results were seen in six experiments and a quantitative analysis of OD value difference was performed in three experiments. The average OD value difference in sites distant from U0126 application is 45.51 ± 5.03, whereas the average OD value difference in the U0126 application sites is 12.18 ± 7.10, indicating the blockade of Arc mRNA localization in the middle molecular layer.

Similar experiments were performed with another MAP kinase kinase (MEK) inhibitor (PD98059), but local delivery of PD98059 through micropipette recording electrodes did not completely block ERK activation in the same way as local delivery of U0126. The incomplete blockade of ERK activation by PD98059 made it impossible to draw strong conclusions, but it was noteworthy that Arc/Arg3.1 mRNA localization was less striking in regions near the PD98059 delivery site (data not shown)

Inhibition of Rho kinase blocks HFS-induced ERK phosphorylation

The data above indicate that blockade of either actin polymerization or ERK phosphorylation prevents the selective targeting of Arc/Arg3.1 mRNA to the activated dendritic domains, suggesting that both are required for selective localization. It was thus of interest to determine whether the two processes were causally linked (that is, whether ERK phosphorylation was required for actin polymerization or vice versa). Phalloidin staining of sections from cases that received U0126 revealed that actin polymerization was not disrupted in areas in which ERK phosphorylation was inhibited (Fig. 8*B*). Thus, actin polymerization does not require ERK activation. Surprisingly, however, p-ERK immunostaining of sections from cases that received the Rho kinase inhibitor revealed that ERK phosphorylation was blocked in the areas (Fig. 8*C*) where actin polymerization was blocked, as evidenced by the absence of a band of phalloidin staining in the middle molecular layer (Fig. 2*C*). Thus, inhibition of Rho kinase blocked the overall activation of ERK in the postsynaptic cells. This finding suggests that ERK activation is downstream of Rho kinase activation or actin polymerization is required for activation of ERK signaling. ERK phosphorylation was also disrupted by local delivery of latrunculin B (Fig. 8*D*). Together, these data support a hypothesis that actin polymerization is also required for ERK activation in response to HFS.

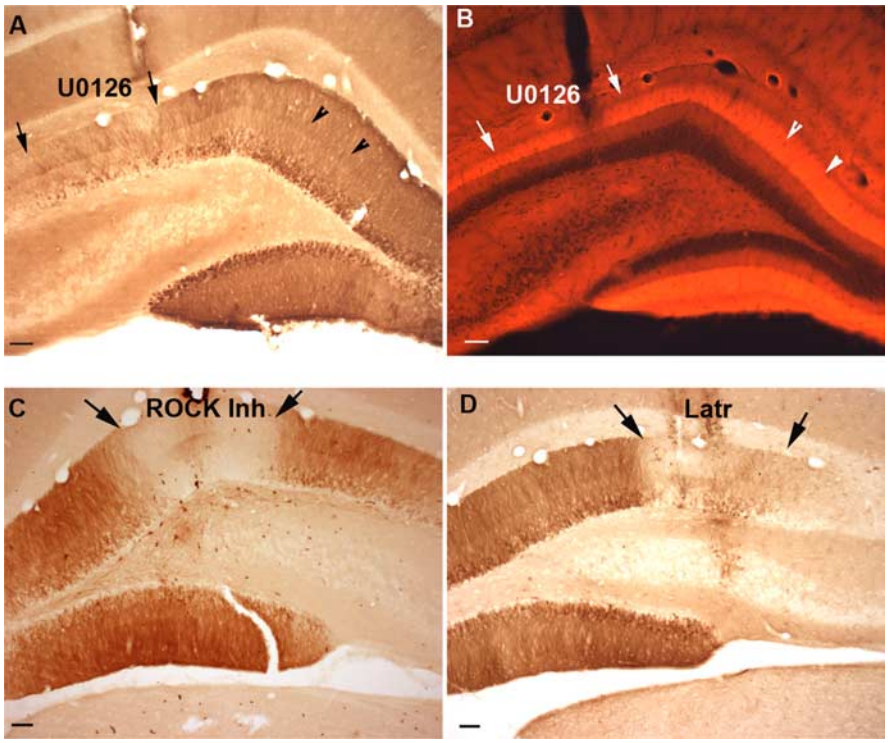

Figure 8. ERK phosphorylation blockade by U0126 has no effect on actin polymerization, but inhibition of actin polymerization inhibition by either the Rho kinase inhibitor or latrunculin B (Latr) blocks ERK phosphorylation. ***A***, ERK phosphorylation is blocked by local application of the MEK inhibitor U0126, as pointed out by arrows. Arrowheads point out site distant from drug application. ***B***, Actin polymerization is not affected by the ERK phosphorylation inhibition. ***C***, ERK phosphorylation is blocked by the Rho kinase inhibitor. ***D***, ERK phosphorylation is blocked by latrunculin B. Arrows point out the drug application site and ERK phosphorylation blockade. Scale bars, 100 μm. The section shown in ***C*** comes from the same case illustrated in Figure 2, *F* and *H* (for the Rho kinase inhibitor).

Discussion

The goal of the present study was to identify components of the mechanism that underlies the targeting of Arc mRNA to active synapses. We show here that strong synaptic stimulation that causes Arc mRNA to localize triggers striking actin polymerization in the activated dendritic lamina. Pharmacological blockade of Rho kinase blocked the development of the band of polymerized actin, and also prevented the localization of Arc/Arg3.1 mRNA to the activated dendritic lamina. The actin polymerization inhibitor latrunculin B had a similar effect, supporting the idea that actin polymerization plays a critical role in Arc mRNA targeting. Nevertheless, the band of polymerized actin is not sufficient to mediate localization. Some other signal is required, and a strong candidate for this secondary signal is ERK phosphorylation in the postsynaptic cytoplasm because inhibition of ERK activation by local injections of the MEK inhibitor U0126 also blocked Arc/Arg3.1 mRNA localization. Together, our findings indicate that both actin polymerization and ERK activation are required for Arc/Arg 3.1 mRNA targeting to the activated dendritic lamina.

Actin polymerization is mediated via NMDA receptor and Rho kinase activation

We show here that actin polymerization induced by HFS depends on NMDA receptor activation, confirming previous studies (Fukazawa et al., 2003), and that actin polymerization depends on Rho kinase. How NMDA receptor activation leads to RhoA–Rho kinase pathway activation to mediate actin polymerization is unclear. Studies of neurons in culture have demonstrated that Lfc, a Rho-specific guanine nucleotide exchange factor, redistributes from microtubules in dendritic shafts to the actin cytoskeleton in dendritic spines after activation of NMDA receptors with glutamate (Ryan et al., 2005). In this way, Ca^{2+} influx via NMDA receptors and L-type Ca^{2+} channels and Lfc translocation to dendritic spines activate RhoA and stabilize F-actin within spines (Ryan et al., 2005).

Molecular participants downstream of Rho kinase also remain to be identified. One possibility is that Rho kinase acts by phosphorylating LIM kinase (LIMK) (Maekawa et al., 1999), which regulates the activity of cofilin/actin depolymerization factor (ADF). Cofilin/ADF can sever F-actin and facilitate actin depolymerization. Phosphorylation of cofilin by LIMK inhibits its activity, which then stabilizes formed F-actin. Consistent with this hypothesis, previous studies have shown that HFS of the perforant path does trigger phosphorylation of LIMK and cofilin (Fukazawa et al., 2003), but direct evidence linking Rho kinase, LIMK phosphorylation, and actin polymerization is lacking.

Arc/Arg3.1 mRNA localization at active synapses: docking or transfer from one transport mechanism to another?

Filamentous actin is enriched in dendritic spines, and the actin cytoskeleton has been shown to be critical for morphological modifications that accompany activity-dependent synaptic plasticity (Luo, 2002; Zhou et al., 2004; Zito et al., 2004; Lippman and Dunaevsky, 2005; Tada and Sheng, 2006). The striking local po-

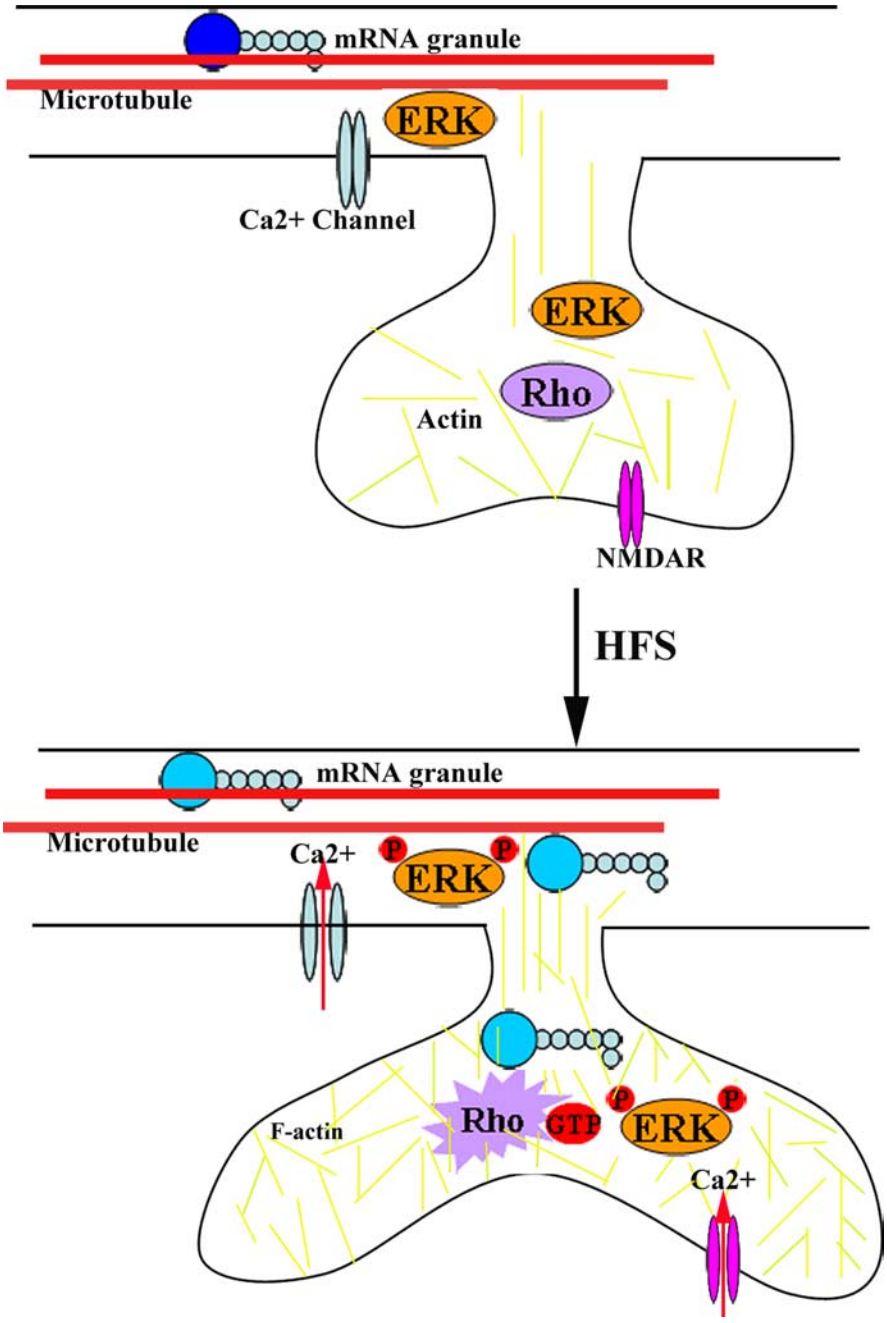

Figure 9. A possible model illustrating the roles of actin polymerization and ERK activation in Arc/Arg3.1 mRNA localization. Under resting conditions (top), NMDAR, Ca^{2+} channels, Rho, and ERK are in an inactive state. RNA granules are being transported along microtubules. After HFS (bottom), NMDA receptor activation triggers actin polymerization in spines, which is mediated by Rho GTPase activation and causes a dramatic alteration in spine morphology. Specifically, the spine neck becomes shorter and wider; the spine head becomes larger and often concave (Fifkova and Anderson, 1981; Desmond and Levy, 1990; Bonhoeffer and Yuste, 2002). More prolonged HFS, as delivered here, accentuates these changes (Steward and Worley, 2001a). HFS activates transcription of Arc/Arg3.1 mRNA, which is then transported into dendrites along microtubules. Actin polymerization in the dendritic spines, when accompanied by ERK activation and maybe other signaling molecules, causes Arc/Arg3.1 mRNA to dissociate from the microtubule-based transport machinery in the dendritic shaft and associate with the modified actin network at the active synapse.

lymerization of actin in the activated dendritic zone reported by Fukazawa et al. (2003) suggested involvement in Arc/Arg3.1 mRNA localization because it occurs selectively in the activated dendritic lamina, and involves a cell-biological mechanism known to be important for short distance transport and/or docking (Lopez de Heredia and Jansen, 2004). We show that blockade of actin polymerization by the Rho kinase inhibitor blocks Arc/Arg3.1 mRNA targeting to the activated dendritic lamina without affecting transcription or Arc/Arg3.1 mRNA transport into dendrites. Similarly, latrunculin B, which inhibits polymerization of actin, blocked the relocalization of Arc/Arg3.1 mRNA to the activated dendritic zone when HFS is delivered after an ECS.

There are two general possibilities for what localization actually involves. NMDA receptor activation may create a signal that propagates through the spine and causes Arc/Arg3.1 mRNA to dissociate from the transport machinery and become stationary (a docking signal). It is believed that mRNA is transported into dendrites in granules, and that this transport depends on microtubules (Kanai et al., 2004). Studies of the movement of Arc/Arg3.1 mRNA granules in living neurons reveal that Arc/Arg3.1 mRNA moves at different rates, with the fastest rate (~60 μm/min) being fast enough to deliver Arc/Arg3.1 from the cell body to the far reaches of distal dendrites within minutes (Dynes and Steward, 2007). When Arc/Arg3.1 is induced in the absence of a localized synaptic signal (for example by a seizure), the mRNA is transported throughout dendrites. Localization occurs when synapses are strongly activated as the mRNA is moving into or through the dendrites. Thus, localization at active synapses requires an interruption of transport, which would require a dissociation of Arc/Arg3.1 mRNA from the microtubule-based transport machinery.

Alternatively, synaptic signals may cause the transfer of Arc/Arg3.1 mRNA from the microtubule-based long-distance transport machinery to a short-distance actin-based transport system that delivers Arc/Arg3.1 into spines. Our data do not allow us to conclude that Arc/Arg3.1 is actually delivered into spine, but there is evidence for a short-distance, spine-specific transport mechanism. For example, polyribosomes redistribute from dendritic shafts into spines during induction of LTP in hippocampal slices (Ostroff et al., 2002). Similarly, after induction of perforant path LTP *in vivo*, mRNAs including calcium-calmodulin-dependent kinase II and Arc/Arg3.1 translocate into spines as revealed by increases in the levels of these mRNAs in isolated synaptoneurosomes (Havik et al., 2003). Also, previous studies have provided evidence that an actin-based motor, myosin-Va, plays a role in Nd1-L messenger ribonucleoprotein (mRNP) translocation from dendrites into spines after activation of mGluRs (Yoshimura et al., 2006). Together, these results suggest that synaptic signals can activate an actin-based local transport mechanism capable of delivering mRNA and ribosomes from the main dendritic shaft into spines.

ERK phosphorylation may create a transient signal for Arc/Arg3.1 mRNA localization at spines with a modified actin cytoskeleton

Our data strongly suggest Arc/Arg3.1 mRNA localization requires actin polymerization, but the band of polymerized actin is not sufficient to cause Arc/Arg3.1 mRNA to localize. This was demonstrated by the experiments in which the band of polymerized actin was induced by HFS, time was allowed for the Arc/Arg3.1 mRNA and protein induced by this stimulation to disappear, and then another wave of Arc/Arg3.1 mRNA expression was triggered by an ECS. In this situation, the Arc/Arg3.1 mRNA synthesized in response to the seizure was transported throughout the dendritic lamina with no hint of selective localization at the band of polymerized actin. These results indicate that the band of polymerized actin is not sufficient to cause Arc mRNA to localize, and that some other signal is required. Moreover, the results indicate that this additional signal diminishes over time after the cessation of stimulation.

If the modification of the actin cytoskeleton is not sufficient to mediate Arc/Arg3.1 mRNA localization, what other signals are required? The obvious possibility is signaling molecules that are transiently activated by HFS and also preferentially localized in the same spatial domain as the band of polymerized actin. The striking phosphorylation of ERK meets these criteria, and a role for p-ERK in Arc/Arg3.1 mRNA localization is further confirmed by the fact that blocking ERK phosphorylation with U0126 abrogates Arc/Arg3.1 mRNA localization. Activated ERK could modify cytoskeletal binding proteins and/or RNA binding proteins to facilitate the capture and anchoring of mRNAs to the actin cytoskeleton in the activated synaptic sites.

A possible role for the actin cytoskeleton in organizing postsynaptic signal transduction cascades

One interesting observation is that inhibition of Rho kinase blocks activity-induced ERK phosphorylation. The same effect is seen with local injections of latrunculin B. There are two possible explanations: ERK activation could be downstream of Rho kinase activation or actin polymerization may be required for activation of MAP kinase signaling. Cross talk between the Rho kinase and MAP kinase cascade is possible, but not well characterized. Alternatively, the actin cytoskeleton could participate in signal transduction by acting as an anchor for postsynaptic macromolecular complexes. Changes in the actin cytoskeleton could thus alter the functional state of postsynaptic proteins, and facilitate signaling pathway activation. Importantly, in other cell types, the actin network plays a critical role in organizing signal transduction networks, especially linkages to membrane receptors, so as to control specificity (Harding et al., 2005).

The local blockade of ERK phosphorylation by the Rho kinase inhibitor and latrunculin B raise one potential confound for the present study. Specifically, one could argue that actin polymerization was required for Arc mRNA localization only by virtue of its role in activating ERK, and that the necessary and sufficient signal was ERK phosphorylation. This is highly unlikely, however, because ERK phosphorylation occurs throughout the postsynaptic cell, and would not provide the spatial specificity that could explain the striking localization of Arc/Arg3.1 mRNA in the activated dendritic lamina. Clearly, some other signal is required to explain the spatial selectivity of the localization, and our findings strongly indicate that it is the local polymerization of actin that provides the spatial selectivity.

In conclusion, we propose that the reorganization of the actin cytoskeleton induced by NMDA receptor activation reflects the activation of an mRNA transport mechanism within activated spines. When coupled with activation of ERK, this spine-specific actin-based transport mechanism delivers Arc/Arg3.1 and perhaps other mRNAs into spines (Fig. 9), and perhaps also mediates the translocation of ribosomes. This delivery is time-limited depending on the duration of ERK activation. The other molecular components of this system (if any) remain to be defined.

References

Allison DW, Gelfand VI, Spector I, Craig AM (1998) Role of actin in anchoring postsynaptic receptors in cultured hippocampal neurons: differential attachment of NMDA versus AMPA receptors. J Neurosci 18:2423–2436.

Bonhoeffer T, Yuste R (2002) Spine motility. Phenomenology, mechanisms, and function. Neuron 35:1019–1027.

Chowdhury S, Shepherd JD, Okuno H, Lyford G, Petralia RS, Plath N, Kuhl D, Huganir RL, Worley PF (2006) Arc/Arg3.1 interacts with the endocytic machinery to regulate AMPA receptor trafficking. Neuron 52:445–459.

Davis S, Vanhoutte P, Pages C, Caboche J, Laroche S (2000) The MAPK/ERK cascade targets both Elk-1 and cAMP response element-binding protein to control long-term potentiation-dependent gene expression in the dentate gyrus *in vivo*. J Neurosci 20:4563–4572.

Desmond NL, Levy WB (1990) Morphological correlates of long-term potentiation imply the modification of existing synapses, not synaptogenesis, in the hippocampal dentate gyrus. Synapse 5:139–143.

Dynes JL, Steward O (2007) Dynamics of bidirectional transport of Arc mRNA in neuronal dendrites. J Comp Neurol 500:433–447.

Fifkova E, Anderson CL (1981) Stimulation-induced changes in dimensions of stalks of dendritic spines in the dentate molecular layer. Exp Neurol 74:621–627.

Fukazawa Y, Saitoh Y, Ozawa F, Ohta Y, Mizuno K, Inokuchi K (2003) Hippocampal LTP is accompanied by enhanced F-actin content within the dendritic spine that is essential for late LTP maintenance *in vivo*. Neuron 38:447–460.

Guzowski JF, McNaughton BL, Barnes CA, Worley PF (1999) Environment-specific expression of the immediate-early gene Arc in hippocampal neuronal ensembles. Nat Neurosci 2:1120–1124.

Guzowski JF, Lyford GL, Stevenson GD, Houston FP, McGaugh JL, Worley PF, Barnes CA (2000) Inhibition of activity-dependent arc protein expression in the rat hippocampus impairs the maintenance of long-term potentiation and the consolidation of long-term memory. J Neurosci 20:3993–4001.

Hall A (1998) Rho GTPases and the actin cytoskeleton. Science 279:509–514.

Harding A, Tian T, Westbury E, Frische E, Hancock JF (2005) Subcellular localization determines MAP kinase signal output. Curr Biol 15:869–873.

Havik B, Rokke H, Bardsen K, Davanger S, Bramham CR (2003) Bursts of high-frequency stimulation trigger rapid delivery of pre-existing alpha-CaMKII mRNA to synapses: a mechanism in dendritic protein synthesis during long-term potentiation in adult awake rats. Eur J Neurosci 17:2679–2689.

Huang F, Chotiner JK, Steward O (2005) The mRNA for elongation factor 1α is localized in dendrites and translated in response to treatments that induce long-term depression. J Neurosci 25:7199–7209.

Kanai Y, Dohmae N, Hirokawa N (2004) Kinesin transports RNA: isolation and characterization of an RNA-transporting granule. Neuron 43:513–525.

Kramar EA, Lin B, Rex CS, Gall CM, Lynch G (2006) Integrin-driven actin polymerization consolidates long-term potentiation. Proc Natl Acad Sci USA 103:5579–5584.

Lin B, Kramar EA, Bi X, Brucher FA, Gall CM, Lynch G (2005) Theta stimulation polymerizes actin in dendritic spines of hippocampus. J Neurosci 25:2062–2069.

Link W, Konietzko U, Kauselmann G, Krug M, Schwanke B, Frey U, Kuhl D (1995) Somatodendritic expression of an immediate early gene is regulated by synaptic activity. Proc Natl Acad Sci USA 92:5734–5738.

Lippman J, Dunaevsky A (2005) Dendritic spine morphogenesis and plasticity. J Neurobiol 64:47–57.

Lopez de Heredia M, Jansen RP (2004) mRNA localization and the cytoskeleton. Curr Opin Cell Biol 16:80–85.

Luo L (2002) Actin cytoskeleton regulation in neuronal morphogenesis and structural plasticity. Annu Rev Cell Dev Biol 18:601–635.

Lyford GL, Yamagata K, Kaufmann WE, Barnes CA, Sanders LK, Copeland NG, Gilbert DJ, Jenkins NA, Lanahan AA, Worley PF (1995) Arc, a growth factor and activity-regulated gene, encodes a novel cytoskeleton-associated protein that is enriched in neuronal dendrites. Neuron 14:433–445.

Maekawa M, Ishizaki T, Boku S, Watanabe N, Fujita A, Iwamatsu A, Obinata T, Ohashi K, Mizuno K, Narumiya S (1999) Signaling from Rho to the actin cytoskeleton through protein kinases ROCK and LIM-kinase. Science 285:895–898.

Matus A, Ackermann M, Pehling G, Byers HR, Fujiwara K (1982) High actin concentrations in brain dendritic spines and postsynaptic densities. Proc Natl Acad Sci USA 79:7590–7594.

Moga DE, Calhoun ME, Chowdhury A, Worley P, Morrison JH, Shapiro ML (2004) Activity-regulated cytoskeletal-associated protein is localized to recently activated excitatory synapses. Neuroscience 125:7–11.

Okamoto K, Nagai T, Miyawaki A, Hayashi Y (2004) Rapid and persistent modulation of actin dynamics regulates postsynaptic reorganization underlying bidirectional plasticity. Nat Neurosci 7:1104–1112.

Ostroff LE, Fiala JC, Allwardt B, Harris KM (2002) Polyribosomes redistribute from dendritic shafts into spines with enlarged synapses during LTP in developing rat hippocampal slices. Neuron 35:535–545.

Plath N, Ohana O, Dammermann B, Errington ML, Schmitz D, Gross C, Mao X, Engelsberg A, Mahlke C, Welzl H, Kobalz U, Stawrakakis A, Fernandez E, Waltereit R, Bick-Sander A, Therstappen E, Cooke SF, Blanquet V, Wurst W, Salmen B, et al. (2006) Arc/Arg3.1 is essential for the consolidation of synaptic plasticity and memories. Neuron 52:437–444.

Rial Verde EM, Lee-Osbourne J, Worley PF, Malinow R, Cline HT (2006) Increased expression of the immediate-early gene arc/arg3.1 reduces AMPA receptor-mediated synaptic transmission. Neuron 52:461–474.

Ryan XP, Alldritt J, Svenningsson P, Allen PB, Wu GY, Nairn AC, Greengard P (2005) The Rho-specific GEF Lfc interacts with neurabin and spinophilin to regulate dendritic spine morphology. Neuron 47:85–100.

Schubert V, Da Silva JS, Dotti CG (2006) Localized recruitment and activation of RhoA underlies dendritic spine morphology in a glutamate receptor-dependent manner. J Cell Biol 172:453–467.

Segal M, Andersen P (2000) Dendritic spines shaped by synaptic activity. Curr Opin Neurobiol 10:582–586.

Shepherd JD, Rumbaugh G, Wu J, Chowdhury S, Plath N, Kuhl D, Huganir RL, Worley PF (2006) Arc/Arg3.1 mediates homeostatic synaptic scaling of AMPA receptors. Neuron 52:475–484.

Steward O, Halpain S (1999) Lamina-specific synaptic activation causes domain-specific alterations in dendritic immunostaining for MAP2 and CAM kinase II. J Neurosci 19:7834–7845.

Steward O, Worley PF (2001a) A cellular mechanism for targeting newly synthesized mRNAs to synaptic sites on dendrites. Proc Natl Acad Sci USA 98:7062–7068.

Steward O, Worley PF (2001b) Selective targeting of newly synthesized *Arc* mRNA to active synapses requires NMDA receptor activation. Neuron 30:227–240.

Steward O, Worley PF (2001c) Localization of mRNAs at synaptic sites on dendrites. Results Probl Cell Differ 34:1–26.

Steward O, Wallace CS, Lyford GL, Worley PF (1998) Synaptic activation causes the mRNA for the IEG Arc to localize selectively near activated postsynaptic sites on dendrites. Neuron 21:741–751.

Tada T, Sheng M (2006) Molecular mechanisms of dendritic spine morphogenesis. Curr Opin Neurobiol 16:95–101.

Tashiro A, Yuste R (2004) Regulation of dendritic spine motility and stability by Rac1 and Rho kinase: evidence for two forms of spine motility. Mol Cell Neurosci 26:429–440.

Tzingounis AV, Nicoll RA (2006) Arc/Arg3.1: linking gene expression to synaptic plasticity and memory. Neuron 52:403–407.

Waltereit R, Dammermann B, Wulff P, Scafidi J, Staubli U, Kauselmann G, Bundman M, Kuhl D (2001) Arg3.1/Arc mRNA induction by Ca^{2+} and cAMP requires protein kinase A and mitogen-activated protein kinase/extracellular regulated kinase activation. J Neurosci 21:5484–5493.

Yoshimura A, Fujii R, Watanabe Y, Okabe S, Fukui K, Takumi T (2006) Myosin-Va facilitates the accumulation of mRNA/protein complex in dendritic spines. Curr Biol 16:2345–2351.

Zhou Q, Homma KJ, Poo MM (2004) Shrinkage of dendritic spines associated with long-term depression of hippocampal synapses. Neuron 44:749–757.

Zito K, Knott G, Shepherd GM, Shenolikar S, Svoboda K (2004) Induction of spine growth and synapse formation by regulation of the spine actin cytoskeleton. Neuron 44:321–334.